X-ray emission processes in stars and their immediate environment

Paola Testa[1]

Smithsonian Astrophysical Observatory, MS-58, 60 Garden Street, Cambridge, MA 02138

A decade of X-ray stellar observations with *Chandra* and *XMM-Newton* has led to significant advances in our understanding of the physical processes at work in hot (magnetized) plasmas in stars and their immediate environment, providing new perspectives and challenges, and in turn the need for improved models. The wealth of high-quality stellar spectra has allowed us to investigate, in detail, the characteristics of the X-ray emission across the Hertzsprung-Russell (HR) diagram. Progress has been made in addressing issues ranging from classical stellar activity in stars with solar-like dynamos (such as flares, activity cycles, spatial and thermal structuring of the X-ray emitting plasma, and evolution of X-ray activity with age), to X-ray generating processes (e.g., accretion, jets, magnetically confined winds) that were poorly understood in the pre*Chandra*/*XMM-Newton* era. I will discuss the progress made in the study of high energy stellar physics and its impact in a wider astrophysical context, focusing on the role of spectral diagnostics now accessible.

activity | spectroscopy | magnetic fields | stellar winds | accretion

In this article I will discuss some recent progress in our understanding of X-ray emission processes in stars, with emphasis towards advances made possible by high-resolution X-ray spectroscopy. This article will necessarily focus on a few selected topics, as tremendous progress has been made in the field in the past decade of *Chandra* and *XMM-Newton* observations, greatly widening our horizons in the study of X-rays from normal stars.

More than half a century of X-ray stellar observations since the first detection of solar X-ray emission (1) have revealed the very rich phenomenology of physical processes at work in the outer atmosphere of stars and their immediate environments. The first systematic observations of X-rays from stars with space observatories revealed that X-ray emission is common in about all types of stars across the Hertzsprung-Russell (HR) diagram though with rather distinct characteristics for different types of stars, pointing to different underlying production mechanisms (2). Most late-type stars are X-ray sources, often highly variable, with levels of X-ray emission spanning more than four orders of magnitude and saturating at a level of fractional X-ray over bolometric luminosity $L_X/L_{bol} \sim 10^{-3}$. The Sun is close to the low activity end of the observed range of X-ray luminosity, with its L_X/L_{bol} ranging between $\sim 10^{-7}$ and $\sim 10^{-6}$ during its activity cycle. Massive stars on the other hand typically show low levels of X-ray variability, and $L_X/L_{bol} \sim 10^{-7}$, consistent with a scenario where X-rays are produced in shocks due to instabilities in the radiatively driven winds (e.g., (3 and 4)). Only in a small range of spectral types, from late B to mid A, are stars observed to be X-ray dark or extremely weak emitters (e.g., (5 and 6)).

Though the basic characteristics of X-ray stellar emission across the HR diagram had been outlined already by previous X-ray observatories, the high sensitivity and spectral resolution of *Chandra* and *XMM-Newton* have provided unique diagnostics which can probe in detail the physics of hot magnetized plasma. These physical processes are also at work in other very different astrophysical environments albeit on very different energy and temporal scales. High-resolution spectroscopy of stars is producing significant unique insights, for instance providing precise temperature and abundance diagnostics, and, for the first time in the X-ray range, diagnostics of density and optical depth.

In the following I will attempt to provide an overview of our current understanding of the X-ray emission mechanisms in massive stars; of the progress in our knowledge of the X-ray activity in solar-like stars; and of selected aspects of the X-ray physics of stars in their early evolution stages in premain sequence. In fact, X-ray stellar studies during this past decade have undergone a shift of focus toward the early phases of stellar evolution and the study of the interplay between circumstellar environment and X-ray activity. E. Feigelson's article in this same issue of PNAS addresses the effects of the X-ray emission from the star on its circumstellar environment, on the evolution of the disk, formation of planets, and planetary atmospheres, which are not discussed in this article.

X-ray Emission in Early-Type Stars: Winds (and Magnetic Fields)

Early findings of approximately constant L_X/L_{bol} for early-type stars, and the low variability of X-ray emission, were well explained by a model in which X-rays originate in shocks produced by instabilities in the radiatively driven winds of these massive stars (e.g., (3 and 4)).

These models yield precise predictions for the shapes and shifts of X-ray emission lines, and models can therefore be tested in detail by deriving information on the line formation radius, overall wind properties, and absorption of overlying cool material. The high spectral resolution of *Chandra* and *XMM-Newton*, and especially the High Energy Transmission Grating Spectrometer (HETGS, (7)) onboard *Chandra* have revealed a much more complex scenario than the standard model described above. In particular, deviations from the standard model seem to suggest that magnetic fields likely play a significant role in some early-type stars. Magnetic fields have in fact recently been detected in a few massive stars (e.g., (8))—most likely fossil fields, because no dynamo mechanism of magnetic field production is predicted to exist for these massive stars since they lack a convective envelope.

High-resolution spectra of several massive stars are mostly consistent with the standard wind-shock model, with soft spectra, and blue-shifted, asymmetric, and broad ($\sim 1,000$ km s^{-1}) emission lines: e.g., ζ Pup (9), ζ Ori (10). Other sources, while characterized by the soft emission predicted by wind-shock models, have spectral line profiles that are rather symmetric, unshifted, and narrow with respect to model expectations: e.g., δ Ori (11), σ Ori (12). Furthermore, a few sources have strong hard X-ray emission with many lines narrower than wind-shock model predictions: e.g., θ^1 Ori C (13), τ Sco (14). For this last class of X-ray sources the presence of magnetic fields provides a plausible explanation for the observed deviations from the wind-shock

model: The magnetic field can confine the wind which yields hotter plasma and narrower lines, as shown for instance for the case of θ^1 Ori C by Gagné et al. through detailed magneto-hydrodynamic simulations which successfully reproduce the observed plasma temperature, L_X, and rotational modulation (13).

An important diagnostic for early-type stars is provided by the He-like triplets (comprising r resonance, i intercombination, and f forbidden lines): The metastable upper level of the f line can be depopulated, populating the upper level of the i transition, through absorption of UV photons. Therefore, the f/i ratio depends on the intensity of the UV field produced by the hot photosphere, i.e., the distance from the photosphere at the location where the given lines form. The f/i ratio is also density sensitive and can be expressed as $R = f/i = R_0/[1 + \phi/\phi_c + n_e/n_c]$, where ϕ_c is a critical value of the UV intensity at the energy coupling the f and i upper levels, and n_c is the density critical value indicating the typical density values at which the f and i upper levels are coupled through collisions; we note however that densities in winds of massive stars are generally expected to be below n_c. The observed He-like line intensities appear to confirm the wind-shock model when the spatial distribution of the X-ray emitting plasma is properly taken into account (15). However there are still unresolved issues. For instance X-ray observations imply opacities that are low and incompatible with the mass loss rates derived otherwise (see ref. 16).

Cool Stars and the Solar Analogy

The Sun, thanks to its proximity, is at present the only star that can be studied at a very high level of detail, with high spatial and temporal resolution, and it is commonly used as a paradigm for the interpretation of the X-ray emission of other late-type stars. However, while the solar analogy certainly seems to apply to some extent to other cool stars, it is not yet well understood how different the underlying processes are in stars with significantly different stellar parameters and X-ray activity levels.

X-ray Activity Cycles. The $\sim$11 yr cycle of activity is one of the most manifest characteristics of the X-ray emission of the Sun, and yet in other stars it is very difficult to observe. This difficulty arises because it is intrinsically challenging to carry out regular monitoring of stellar X-ray emission over long enough time scales, and to confidently identify long term cyclic variability from short term variations that are not unusual in cool stars (e.g., flares, rotational modulation). Long term systematic variability similar to the Sun's cycle has now been observed in three solar-like stars: HD 81809 (spectral type G5V, (17)), 61 Cyg A (K5V, (18)), α Cen A (G2V, (19)). The existence of X-ray cycles in other stars confirms the solar-stellar analogy, and it is also potentially useful in order to better understand the dynamo activity on the Sun, which remains a significant challenge.
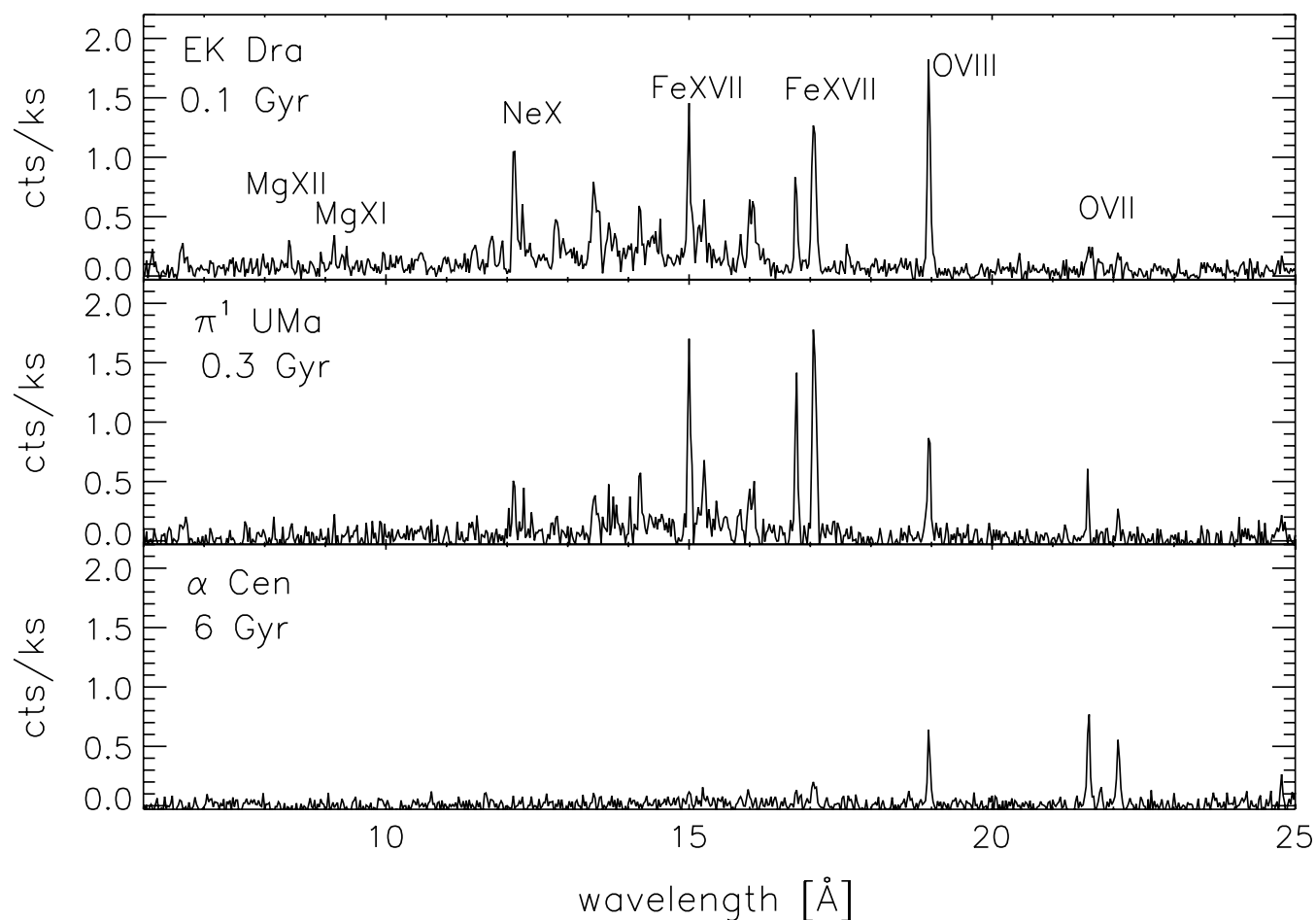
Fig. 1. X-ray *Chandra* Low Energy Transmission Grating spectra of solar-like stars at different ages, showing the evolution of the X-ray spectrum from an age of $\sim$100 Myr to $\sim$6 Gyr. From *top to bottom*: EK Dra – age $\sim$ 100 Myr, $P_{rot} \sim$ 2.7 d, $M_\star \sim 0.9 M_\odot$ (observation identification number, ObsID: 1884; exposure time 66 ks); π^1 UMa – age $\sim$ 300 Myr, $P_{rot} \sim$ 4.7 d, $M_\star \sim 1 M_\odot$ (ObsID: 23; 30 ks); α Cen – age $\sim$ 6 Gyr, $P_{rot} \sim P_\odot$ (i.e., $\sim$27 d), $M_\star \sim 1.1 M_\odot$ (ObsID: 7432; 117 ks). Some of the strongest lines are labeled in the spectrum of EK Dra. The intensity of O VIII emission relative to O VII provides a visual indication of the temperature of the X-ray emitting plasma, being larger for higher temperatures. Younger solar-like stars are characterized by higher X-ray emission levels ($L_X \gtrsim 10^{30}$ erg s^{-1}, i.e., $\gtrsim 10^3 (L_X)_\odot$), coronal temperatures ($T \gtrsim$ 10 MK), and flaring rates. These all decrease with age because of the reduced efficiency of the underlying dynamo mechanism at the lower rotation rates due to substantial angular momentum loss.
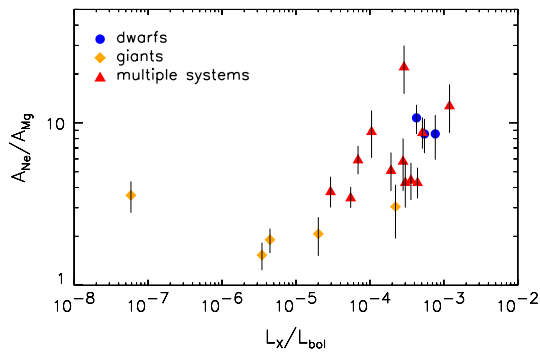
Fig. 2. Abundance ratio of high FIP Ne to low FIP Mg for a sample of stars covering a wide range of activity. The abundance ratio is derived through a ratio of combination of H-like and He-like resonance lines, which is optimized to make the ratio largely temperature insensitive, as in (27). The sample of spectra is the same analyzed by Drake & Testa (27).

The Sun in Time. Studies of large samples of solar-like stars at different evolutionary stages help investigate the evolution of the dynamo processes that are mainly responsible for the X-ray production in these cool stars. In particular, studies of this type carried out with high-resolution spectroscopy, while requiring a large investment of time and therefore focusing necessarily on small samples of stars, have nonetheless provided very important insights into the response of the corona to the decline in rotation-powered magnetic field generation and dissipation, and provided details of how X-ray emission on the Sun has evolved over time, as shown for instance by Telleschi et al. (20). The evolution of the solar coronal emission in time could, in turn, be relevant to the evolution of the solar system and the earth's atmosphere (see E. Feigelson's article in this same issue of PNAS). Within relatively short timescales, during the post T Tauri through early main sequence phase, the efficient mass loss spins down the star significantly. This process affects the dynamo mechanism because the stellar rotation rate is one of the most important parameters driving the dynamo. As a consequence, the X-ray activity decreases, with coronal temperature, L_X, and flare rate all decreasing, as shown in Fig. 1 for three solar-like stars spanning ages from ~100 Myr to ~6 Gyr.

Element Abundances. The study of element abundances has important implications in the wider astrophysical context and also for stellar physics. For instance, chemical composition is a fundamental ingredient for models of stellar structure since it significantly impacts the opacity of the plasma. Spectroscopic studies of the solar corona have provided a robust body of evidence for element fractionation with respect to the photospheric composition (see ref. 21 and references therein). Furthermore, this fractionation effect appears to be a function of the element First Ionization Potential (FIP), with low FIP elements such as Fe, Si, and Mg, found to be enhanced in the solar corona by a factor of a few, while high FIP elements such as O have coronal abundances close to their photospheric values (e.g., (21)). This "FIP effect" has strong implications for the physical processes at work in the solar atmosphere (see refs. 22 and 23 and references therein). Spectroscopic studies in the extreme ultraviolet have provided the first indication that in other stars as well the chemical composition of coronal plasma is different from that of the underlying photosphere, although with a dependence on FIP that is likely significantly different from that on the Sun (e.g., (24)). High-resolution X-ray spectroscopy with *Chandra* and *XMM-Newton* has for the first time provided robust and detailed information on the chemical composition patterns of hot coronal plasma. Stellar coronae at the high end of the X-ray activity range appear characterized by an *inverse* FIP effect (IFIP), i.e., with Fe and other low FIP elements significantly depleted in the corona, compared

to the high FIP elements like oxygen (e.g., (25)). Investigation of element abundances in large samples of stars spanning a large range of activity ($L_X/L_{bol} \sim 10^{-6} - 10^{-3}$) finds a systematic gradual increase of IFIP effect with activity level (e.g.,(26)). This trend is shown in Fig. 2 for the abundance ratio of low FIP element Mg to high FIP element Ne, derived from *Chandra* HETGS spectra for the same sample of stars for which Drake & Testa studied the Ne/O abundance ratio (27). An important caveat to keep in mind is that the stellar photospheric chemical composition is often unknown for the elements of interest, and the **solar** photospheric composition is instead used as a reference (28).

In this context an interesting result is the behavior of Ne/O which remains rather constant over almost the whole observed range of activity (27), and, interestingly, this almost constant value is about 2.7 times higher than the adopted solar photospheric value. This finding might help to shed light on an outstanding puzzle in our understanding of our own Sun. Since Ne cannot be measured in the photosphere—no photospheric Ne lines are present in the solar spectrum—the solar photospheric Ne/O is not constrained. The remarkably constant Ne/O observed in stellar coronae, despite the significantly different properties of these stars, suggests that the observed coronal Ne/O actually reflects the underlying photospheric abundances. If the same value is assumed for the solar photosphere as well, this would help resolve a troubling inconsistency between solar models and data from helioseismology observations (29). It remains unresolved though why the solar coronal Ne/O is found to be systematically lower than in other coronae (e.g., (30)), though this is likely similar to other low activity stars (31). However, Laming (23) suggests that the low coronal Ne abundance on the Sun might be explained by the same fractionation processes that yield the general FIP effect.

Spatial Structuring of X-ray Emitting Plasma and Dynamic Events. High spectral resolution in X-rays has made accessible a whole new range of possible diagnostics for the spatial structuring of stellar coronae, for example:

- **opacity** effects in strong resonance lines yield estimates of path length, and therefore the spatial extent of X-ray emitting structures. Only a handful of sources show scattering effects in their strongest lines, and the derived lengths are very small when compared to the stellar radii, analogous to solar coronal structures (32–34).
- **velocity modulation** derived from line shifts allows us to estimate the spatial distribution of the X-ray emitting plasma at different temperatures, or the contribution of multiple system components to the total observed emission (e.g., (35–39)). The unprecedented high spectral resolution of *Chandra* is crucial for these studies with a velocity resolution down to ~30 km s^{-1} (e.g., (37, 38, 40)).
- **plasma density**, n_e, can be derived from the ratios of He-like triplets ($R = f/i \sim R_0/[1 + n_e/n_c]$; (41))*, therefore providing an estimate of the emitting volumes, because the observed line intensity is proportional to $n_e^2 V$. Several He-like triplet lines lie in the *Chandra* and *XMM-Newton* spectral range covering a wide range of temperatures (~3–10 MK from O VII to Si XIII), and densities ($\log(n_c[\text{cm}^{-3}]) \sim 10.5$–13.5 from O VII to Si XIII). We note that the unmatched resolving power of *Chandra* HETGS is crucial to resolve the numerous blends that affect the Ne and Mg triplets that cover the important ~3–6 × 10^6 K range. Studies of plasma densities from He-like triplets in large samples of stars ((42) studied O VII, Mg XII, Si

---

*For cool stars the UV field is typically too weak to affect the He-like lines (which it does for hot stars as mentioned above) and therefore the f/i ratio is mainly sensitive to the plasma density, above a critical density value which depends on the specific triplet (see (41)).

XIII, and (43) O VII and Ne IX) yield estimates of coronal filling factors which are remarkably small especially for hotter plasma (typically $\ll 1$), but increase with X-ray surface flux (42).

- **flares** can provide clues on the size of the X-ray emitting structures and on the underlying physical processes that produce very dynamic events. The timescale of evolution of the flaring plasma (T, n_e) is related to the size of the flaring structure(s), and can be modeled to provide constraints on the loop size (see ref. 44 and references therein). Flares we observe in active stars involve much larger amounts of energy than observed on the Sun, with X-ray luminosities reaching values of 10^{32} erg s^{-1} and above, i.e., more than two orders of magnitude larger than the most powerful solar flares. It is therefore not obvious that these powerful stellar flares are simply scaled up (L_X, T, characteristic timescales of evolution) versions of solar flares which we can study and model with a much higher level of detail. Unique diagnostics are provided by high-resolution spectra, and time-resolved high-resolution spectroscopy of stellar flares is now possible with *Chandra* and *XMM-Newton*, at least for large flares in bright nearby sources. For instance, Güdel et al. (45) have studied a large flare observed on Proxima Centauri, finding evidence of phenomena analogous to solar flaring events: density enhancement during the flare, supporting the scenario of chromospheric evaporation, and the Neupert effect, i.e., proportionality between soft X-ray emission and the integral of the nonthermal emission (e.g., (46)). An interesting, and potentially powerful unique diagnostic is provided by Fe Kα (6.4 keV, 1.94 Å) emission, which can be observed in *Chandra* and *XMM-Newton* spectra. On the Sun, Fe Kα emission has been observed during flares (e.g., (47)) and it is interpreted as **fluorescence** emission following inner shell ionization of *photospheric* neutral Fe due to hard X-ray coronal emission (>7.11 keV). In this scenario, the efficiency of Fe Kα production depends on the geometry, i.e., on the height of the source of hard ionizing continuum, through the dependence on the solid angle subtended and the average depth of formation of Fe Kα photons (e.g., (48 and 49)). In cool stars other than the Sun, Fe Kα has now been detected in young stars with disks (see *Young Stars: Powerful Coronae, Accretion, Jets, Magnetic Fields and Winds*) where the fluorescent emission is thought to come from the cold disk material, and in only two, supposedly diskless, sources during large flares: the G1 yellow giant HR 9024 (50), and the RS CVn system II Peg (51 and 52). For HR 9024 the *Chandra* HETGS observations can be matched in detail with a hydrodynamic model of a flaring loop yielding an estimate for the loop height $h \sim 0.3R_\star$ (53), and an *effective height* for the fluorescence production of $\sim 0.1R_\star$ ($R_\star$ being the stellar radius). These values compare well with the value derived from the analysis of the measured Fe Kα emission, $h \lesssim 0.3R_\star$.

Young Stars: Powerful Coronae, Accretion, Jets, Magnetic Fields and Winds

X-ray emission from young stars is presently one of the hot topics in X-ray astrophysics. Stellar X-rays are thought to significantly affect the dynamics, heating, and chemistry of protoplanetary disks, influencing their evolution (see E. Feigelson's article in this same issue of PNAS). Also, irradiation of close-in planets increases their mass loss rates possibly to the extent of complete evaporation of their atmospheres (e.g., (54)).

Young stars are typically characterized by strong and variable X-ray emission (e.g., (55)), and many recent *Chandra* and *XMM-Newton* studies have been investigating whether their coronae might just be powered up versions of their evolved main sequence counterparts, or whether other processes might be at work in these early evolutionary stages. For example, the observations have addressed the issue of accretion-related X-ray emission processes in accreting (classical) T Tauri stars (CTTS), on which
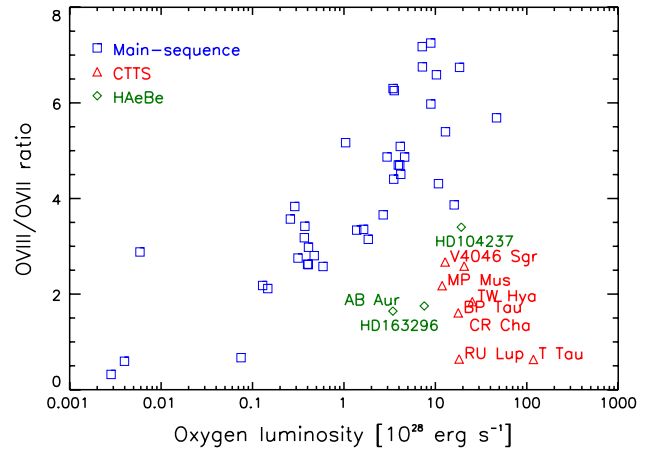
Fig. 3. The ratio of O VIII/O VII vs. oxygen luminosity for a large sample of main sequence and premain sequence stars shows the soft excess in high-resolution spectra of CTTS and HAe stars with respect to main sequence and nonaccreting stars. Modified from ref. 77, where the data point for HD 104237 [using measured fluxes from (78)] has been added; reproduced with permission, copyright ESO.

material from a circumstellar disk is channeled onto the central star by its magnetic field.

CTTS have observed X-ray luminosities that are systematically smaller by about a factor two than nonaccreting TTS, (e.g., (55)). It is not yet clear however if accretion might suppress or obscure coronal X-rays, or instead, whether higher X-ray emission levels might increase photoevaporation of the accreting material, modulating the accretion rate (56).

Accretion-Related X-ray Production. High-resolution spectroscopy has proved crucial for probing the physics of X-ray emission processes in young stars. The first high-resolution X-ray spectrum of an accreting TTS, TW Hya, has revealed obvious peculiarities (57) with respect to the coronal spectra of main sequence cool stars:

- **very soft emission**: The X-ray spectrum of TW Hya is characterized by a temperature of only few MK (~ 3 MK), whereas coronae with comparable X-ray luminosities ($L_X \sim 10^{30}$ erg s^{-1}) typically have strong emission at temperatures $\gtrsim 10$ MK.
- **high n_e**: The strong cool He-like triplets of Ne and O have line ratios that imply very high densities ($n_e \gtrsim 10^{12}$ cm^{-3}), whereas in nonaccreting sources typical densities are about two orders of magnitude lower.
- **abundance anomalies**: The X-ray spectrum of TW Hya is characterized by very low metal abundances, while Ne is extremely high (58 and 59) when compared to other stellar coronae.

These peculiar properties strongly suggest that the X-ray emission of TW Hya is originating from shocked accreting plasma. Indeed, the observed X-ray spectra of some of these sources have been successfully modeled as accretion shocks (60 and 61). High-resolution spectra subsequently obtained for other CTTS have confirmed unusually high n_e from the O VII lines (62–65), indicating that in these stars at least some of the observed X-rays are most likely produced through accretion-related mechanisms. We note that TW Hya is the CTTS for which the cool X-ray emission produced in the accretion shocks is the most prominent with respect to the coronal emission, while all other CTTS for which high-resolution spectra have been obtained have a much stronger coronal component. For these latter sources we are able to probe accretion-related X-rays only thanks to the high spectral resolution which allows us to separate the two components. Recent

studies of optical depth effect in strong resonance lines in CTTS provide confirmation of the high densities derived from the He-like diagnostics (66). Another diagnostic of accretion-related X-ray production mechanisms is offered by the O VIII/O VII ratio which, in accreting TTS, is much larger than in nonaccreting TTS or main sequence stars (67) (see also Fig. 3). Herbig AeBe stars, young intermediate mass analogs of TTS, appear to share the same properties (65).

Flaring Activity and Coronal Geometry. X-ray emission of young stars is characterized by very high levels of X-ray variability pointing to very intense flaring activity in the young coronae of TTS. This is beautifully demonstrated by the *Chandra* Orion Ultradeep Project of almost uninterrupted (spanning about 13 d) observations of the Orion Nebula Cluster star forming region [†]. Hydrodynamic modeling of some of the largest flares of TTS imply, for some of these sources, very large sizes for the flaring structures ($L \gtrsim 10R_\star$). This finding may provide evidence of a star-disk connection (68). However, follow-up studies of these flares indicate that the largest structures seem to be associated with nonaccreting sources, consistent with the idea that in accreting sources, the inner disk reaching close to the star, might truncate the otherwise very large coronal structures (69). In a few of these sources, with strong hard X-ray spectra, Fe Kα emission has been observed (see ref. 70 for a survey of Orion stars). The Fe Kα emission is generally interpreted as fluorescence from the circumstellar disk, however in a few cases the observed equivalent widths are extremely high and apparently incompatible with fluorescence models (see refs. 71 and 72). This apparent discrepancy could either be due to partial obscuration of the X-ray emission of the flare (49) or could instead point to different physical processes at work, for instance impact excitation (73).

Herbig Ae Stars. In their premain sequence phase, intermediate mass stars appear to be moderate X-ray sources (e.g., (74) and references therein). Their X-ray emission characteristics are overall similar to the lower mass TTS (hot, variable), possibly implying that the same X-ray emission processes are at work in the two classes of stars or that the emission is due to unseen TTS companions. However, a handful of Herbig Ae stars show unusually soft X-ray emission: e.g., AB Aur (75), HD 163296 (76 and 77). High-resolution spectra have been obtained for these stars, together with HD 104237 (78). One similarity with the high-resolution spectra of CTTS, appears to be the presence of a soft excess (O VIII/O VII), compared to coronal sources, as shown by (77) (see Fig. 3). However their He-like triplets are generally compatible with low density, at odds with the accreting TTS (with maybe the exception of HD 104237, possibly indicating higher n_e). AB Aur and HD 104237 have X-ray emission that seems to be modulated on timescales comparable with the rotation period of the A-type star therefore rendering the hypothesis that X-ray emission originates from low-mass companions less plausible.

Conclusions

The past decade of stellar observations has led to exciting progress in our understanding of the X-ray emission processes in stars, also shifting in the process the perspective of stellar studies which are now much more focused on star and planet formation. In particular high-resolution X-ray spectroscopy, available with *Chandra* and *XMM-Newton*, is now playing a crucial role in constraining and developing models of X-ray emission, e.g., for early type stars, late-type stellar coronae, and in the case of young stars, by providing a unique means for probing accretion-related X-ray emission processes, as well as the opportunity to examine the effects of X-rays on the circumstellar environment.

Progress and some open issues in X-ray emission processes: X-ray emission processes in early type stars now present a much more complex scenario in which magnetic fields also likely play a key role. Some puzzling results found for several massive stars concern the hard, variable X-ray spectra with relatively narrow lines, which cannot be explained by existing models.

Spectroscopic studies of large samples of stars have provided robust findings on chemical fractionation in X-ray emitting plasma, which now require improved models to understand the physical processes yielding the observed abundance anomalies.

A satisfactory understanding of activity cycles is lacking even for our own Sun, and recent discoveries of X-ray cycles on other stars can provide further constrains for dynamo models.

We are now taking the first steps in studying flares with temporally resolved high-resolution spectra, and this will greatly help constrain our models and really test whether the physics of these dynamic events, in the extreme conditions seen in some cases (e.g., $T \gtrsim 10^8$ K), are still the same as for solar flares. At present, the effective areas are often insufficient to obtain good signal-to-noise at high spectral resolution on the typical timescales of the plasma evolution during these very dynamic events. The International X-ray Observatory, in the planning stages for a launch about a decade from now, will make a large number of stars accessible for this kind of study.

In young stars, a very wide range of phenomena are observed to occur, and while this young field has already offered real breakthroughs there is still a long way to go to understand the details of accretion, jets, extremely large X-ray emitting structures, the influence of X-rays on disks and planets, and the interplay between accretion and X-ray activity.

1. Friedman H, Lichtman SW, Byram ET (1951) Photon counter measurements of solar X-rays and extreme ultraviolet light. *Physical Review* 83:1025–1030.
2. Vaiana GS, et al. (1981) Results from an extensive Einstein stellar survey. *The Astrophysical Journal* 245:163–182.
3. Lucy LB, White RL (1980) X-ray emission from the winds of hot stars. *The Astrophysical Journal* 241:300–305.
4. Owocki SP, Castor JI, Rybicki GB (1988) Time-dependent models of radiatively driven stellar winds. I—Nonlinear evolution of instabilities for a pure absorption model. *The Astrophysical Journal* 335:914–930.
5. Czesla S, Schmitt JHHM (2007) Are magnetic hot stars intrinsic X-ray sources?. *Astronomy and Astrophysics* 465:493–499.
6. Schröder C, Schmitt JHHM (2007) X-ray emission from A-type stars. *Astronomy and Astrophysics* 475:677–684.
7. Canizares CR, et al. (2005) The *Chandra* high-energy transmission grating: Design, fabrication, ground calibration, and 5 years in flight. *The Publications of the Astronomical Society of the Pacific* 117:1144–1171.
8. Donati JF, et al. (2002) The magnetic field and wind confinement of θ¹ Orionis C. *Monthly Notices of the Royal Astronomical Society* 333:55–70.
9. Cassinelli JP, Miller NA, Waldron WL, MacFarlane JJ, Cohen DH (2001) *Chandra* detection of doppler-shifted X-ray line profiles from the wind of ζ puppis (O4 F). *The Astrophysical Journal Letters* 554:55–58.
10. Cohen DH, et al. (2006) Wind signatures in the X-ray emission-line profiles of the late-O supergiant ζ Orionis. *Monthly Notices of the Royal Astronomical Society* 368:1905–1916.
11. Miller NA, Cassinelli JP, Waldron WL, MacFarlane JJ, Cohen DH (2002) New challenges for wind shock models: the *Chandra* spectrum of the hot star δ Orionis. *The Astrophysical Journal* 577:951–960.
12. Skinner SL, et al. (2008) High-resolution *Chandra* X-ray imaging and spectroscopy of the σ Orionis cluster. *The Astrophysical Journal* 683:796–812.
13. Gagné M, et al. (2005) *Chandra* HETGS multiphase spectroscopy of the young magnetic O star θ¹ Orionis C. *The Astrophysical Journal* 628:986–1005.
14. Cohen DH, et al. (2003) High-resolution *Chandra* spectroscopy of τ Scorpii: A narrow-line X-ray spectrum from a hot star. *The Astrophysical Journal* 586:495–505.
15. Leutenegger MA, Paerels FBS, Kahn SM, Cohen DH (2006) Measurements and analysis of Helium-like triplet ratios in the X-ray spectra of O-type stars. *The Astrophysical Journal* 650:1096–1110.

[†]Movies of this dataset are available at http://www.astro.psu.edu/coup/.

Testa

16. Owocki SP, Cohen DH (2001) X-ray line profiles from parameterized emission within an accelerating stellar wind. *The Astrophysical Journal* 559:1108–1116.

17. Favata F, Micela G, Orlando S, Schmitt JHMM, Sciortino S (2008) The X-ray cycle in the solar-type star HD 81809. XMM-Newton observations and implications for the coronal structure. *Astronomy and Astrophysics* 490:1121–1126.

18. Hempelmann A, et al. (2006) Coronal activity cycles in 61 Cygni. *Astronomy and Astrophysics* 460:261–267.

19. Ayres TR (2009) The cycles of α Centauri. *The Astrophysical Journal* 696:1931–1949.

20. Telleschi A, et al. (2005) Coronal evolution of the Sun in time: high-resolution X-ray spectroscopy of solar analogs with different ages. *The Astrophysical Journal* 622:653–679.

21. Feldman U (1992) Elemental abundances in the upper solar atmosphere. *Physica Scripta* 46(3):202–220.

22. Laming JM (2004) A unified picture of the first ionization potential and inverse first ionization potential effects. *The Astrophysical Journal* 614:1063–1072.

23. Laming JM (2009) Non-Wkb models of the first ionization potential effect: implications for solar coronal heating and the coronal Helium and Neon abundances. *The Astrophysical Journal* 695:954–969.

24. Drake JJ, Laming JM, Widing KG (1996) The FIP effect and abundance anomalies in late-type stellar coronae. *IAU Colloq*, eds S Bowyer and RF Malina 97.

25. Brinkman AC, et al. (2001) First light measurements with the XMM-Newton reflection grating spectrometers: Evidence for an inverse first ionisation potential effect and anomalous Ne abundance in the Coronae of HR 1099. *The Astrophysical Journal Letters* 365:653–679.

26. García-Alvarez D, Drake JJ, Kashyap VL, Lin L, Ball B (2008) Coronae of young fast rotators. *The Astrophysical Journal* 679:1509–1521.

27. Drake JJ, Testa P (2005) The "solar model problem" solved by the abundance of neon in nearby stars. *Nature* 436:525–528.

28. Sanz-Forcada J, Favata F, Micela G (2004) Coronal versus photospheric abundances of stars with different activity levels. *Astronomy and Astrophysics* 416:281–290.

29. Antia HM, Basu S (2005) The discrepancy between solar abundances and helioseismology. *The Astrophysical Journal Letters* 620:129–132.

30. Young PR (2005) The Ne/O abundance ratio in the quiet Sun. *Astronomy and Astrophysics* 444:L45–L48.

31. Robrade J, Schmitt JHMM, Favata F (2008) Neon and oxygen in low activity stars: towards a coronal unification with the Sun. *Astronomy and Astrophysics* 486:995–1002.

32. Testa P, Drake JJ, Peres G, DeLuca EE (2004) Detection of X-ray resonance scattering in active stellar coronae. *The Astrophysical Journal Letters* 609:L79–L82.

33. Matranga M, Mathioudakis M, Kay HRM, Keenan FP (2005) Flare X-ray observations of AB Doradus: evidence of stellar coronal opacity. *The Astrophysical Journal Letters* 621:L125–L128.

34. Testa P, Drake JJ, Peres G, Huenemoerder DP (2007) On X-ray optical depth in the coronae of active stars. *The Astrophysical Journal* 665:1349–1360.

35. Brickhouse NS, Dupree AK, Young PR (2001) X-ray doppler imaging of 44i Bootis with *Chandra. The Astrophysical Journal Letters* 562:75–78.

36. Chung SM, Drake JJ, Kashyap VL, Lin L, Ratzlaff PW (2004) Doppler shifts and broadening and the structure of the X-ray emission from Algol. *The Astrophysical Journal* 606:1184–1195.

37. Ishibashi K, Dewey D, Huenemoerder DP, Testa P (2006) *Chandra*/HETGS observations of the Capella system: the primary as a dominating X-ray source. *The Astrophysical Journal Letters* 644:L117–L120.

38. Huenemoerder DP, Testa P, Buzasi DL (2006) X-ray spectroscopy of the contact binary VW Cephei. *The Astrophysical Journal* 650:1119–1132.

39. Hussain GAJ, et al. (2007) The coronal structure of AB Doradus determined from contemporaneous Doppler imaging and X-ray spectroscopy. *Monthly Notices of the Royal Astronomical Society* 377:1488–1502.

40. Hoogerwerf R, Brickhouse NS, Mauche CW (2004) The radial velocity and mass of the white dwarf of EX Hydrae measured with *Chandra. The Astrophysical Journal* 610:411–415.

41. Gabriel AH, Jordan C (1969) Interpretation of solar helium-like ion line intensities. *Monthly Notices of the Royal Astronomical Society* 145:241–248.

42. Testa P, Drake JJ, Peres G (2004) The density of coronal plasma in active stellar coronae. *The Astrophysical Journal* 617:508–530.

43. Ness J-U, Güdel M, Schmitt JHMM, Audard M, Telleschi A (2004) On the sizes of stellar X-ray coronae. *Astronomy and Astrophysics* 427:667–683.

44. Reale F (2007) Diagnostics of stellar flares from X-ray observations: from the decay to the rise phase. *Astronomy and Astrophysics* 417:271–279.

45. Güdel M, Audard M, Skinner SL, Horvath MI (2002) X-ray evidence for flare density variations and continual chromospheric evaporation in Proxima Centauri. *The Astrophysical Journal Letters* 580:L73–L76.

46. Hudson HS, Acton LW, Hirayama T, Uchida Y (1992) White-light flares observed by YOHKOH. *The Publications of the Astronomical Society of the Pacific* 44:L77–L81.

47. Parmar AN, et al. (1984) SMM observations of K-α radiation from fluorescence of photospheric iron by solar flare X-rays. *The Astrophysical Journal* 279:866–874.

48. Bai T (1979) Iron K-α fluorescence in solar flares—A probe of the photospheric iron abundance. *Sol Phys* 62:113–121.

49. Drake JJ, Ercolano B, Swartz DA (2008) X-ray-fluorescent Fe Kα lines from stellar photospheres. *The Astrophysical Journal* 678:385–393.

50. Testa P, et al. (2008) Geometry diagnostics of a stellar flare from fluorescent X-rays. *The Astrophysical Journal Letters* 675:L97–L100.

51. Osten RA, et al. (2007) Nonthermal hard X-ray emission and iron Kαemission from a superflare on II Pegasi. *The Astrophysical Journal* 654:1052–1067.

52. Ercolano B, Drake JJ, Reale F, Testa P, Miller JM (2008) Fe Kα and hydrodynamic loop model diagnostics for a large flare on II Pegasi. *The Astrophysical Journal* 688:1315–1319.

53. Testa P, Reale F, Garcia-Alvarez D, Huenemoerder DP (2007) Detailed diagnostics of an X-ray flare in the single giant HR 9024. *The Astrophysical Journal* 663:1232–1243.

54. Penz T, Micela G, Lammer H (2008) Influence of evolving stellar X-ray luminosity distribution on exoplanetary mass loss. *Astronomy and Astrophysics* 477:309–314.

55. Preibisch T, et al. (2005) The origin of T Tauri X-ray emission: new insights from the *Chandra* Orion Ultradeep Project. *The Astrophysical Journal Supplement Series* 160:401–422.

56. Drake JJ, Ercolano B, Flaccomio E, Micela G (2009) X-ray photoevaporation-starved T Tauri accretion. *The Astrophysical Journal Letters* 699:35–38.

57. Kastner JH, Huenemoerder DP, Schulz NS, Canizares CR, Weintraub DA (2002) Evidence for accretion: high-resolution X-ray spectroscopy of the classical T Tauri star TW Hydrae. *The Astrophysical Journal* 567:434–440.

58. Stelzer B, Schmitt JHHM (2004) X-ray emission from a metal depleted accretion shock onto the classical T Tauri star TW Hya. *Astronomy and Astrophysics* 418:687–697.

59. Drake JJ, Testa P, Hartmann L (2005) X-ray diagnostics of grain depletion in matter accreting onto T Tauri stars. *The Astrophysical Journal Letters* 627:149–152.

60. Günther HM, Schmitt JHHM, Robrade J, Liefke C (2007) X-ray emission from classical T Tauri stars: accretion shocks and coronae?. *Astronomy and Astrophysics* 466:1111–1121.

61. Sacco GG, et al. (2008) X-ray emission from dense plasma in classical T Tauri stars: hydrodynamic modeling of the accretion shock. *Astronomy and Astrophysics* 491:L17–L20.

62. Schmitt JHHM, Robrade J, Ness JU, Favata F, Stelzer B (2005) X-rays from accretion shocks in T Tauri stars: The case of BP Tau. *Astronomy and Astrophysics* 432:L35–L38.

63. Günther HM, Liefke C, Schmitt JHHM, Robrade J, Ness JU (2006) X-ray accretion signatures in the close CTTS binary V4046 Sagittarii. *Astronomy and Astrophysics* 459:L29–L32.

64. Argiroffi C, Maggio A, Peres G (2007) X-ray emission from MP Muscae: an old classical T Tauri star. *Astronomy and Astrophysics* 465:5–8.

65. Robrade J, Schmitt JHHM (2007) X-rays from RU Lupi: accretion and winds in classical T Tauri stars. *Astronomy and Astrophysics* 473:229–238.

66. Argiroffi C, et al. (2009) X-ray optical depth diagnostics of T Tauri accretion shocks. *Astronomy and Astrophysics* 507:939–948.

67. Güdel M, Telleschi A (2007) The X-ray soft excess in classical T Tauri stars. *Astronomy and Astrophysics* 474:L25–L28.

68. Favata F, et al. (2005) Bright X-ray flares in Orion young stars from COUP: evidence for star-disk magnetic fields?. *The Astrophysical Journal Supplement Series* 160:469–502.

69. Getman KV, et al. (2008) X-ray flares in Orion young stars. II. Flares, magnetospheres, and protoplanetary disks. *The Astrophysical Journal* 688:437–455.

70. Tsujimoto M, et al. (2005) Iron fluorescent line emission from young stellar objects in the Orion Nebula. *The Astrophysical Journal Supplement Series* 160:503–510.

71. Czesla S, Schmitt JHHM (2007) The nature of the fluorescent iron line in V 1486 Orionis. *Astronomy and Astrophysics* 470:L13–L16.

72. Giardino G, et al. (2007) Results from Droxo. I. The variability of fluorescent Fe 6.4 keV emission in the young star Elias 29. High-energy electrons in the star's accretion tubes?. *Astronomy and Astrophysics* 475:891–900.

73. Emslie AG, Phillips KJH, Dennis BR (1986) The excitation of the iron K-α feature in solar flares. *Sol Phys* 103:89–102.

74. Stelzer B, Robrade J, Schmitt JHHM, Bouvier J (2009) New X-ray detections of Herbig stars. *Astronomy and Astrophysics* 493:1109–1119.

75. Telleschi A, et al. (2007) The first high-resolution X-ray spectrum of a Herbig: AB Aurigae. *Astronomy and Astrophysics* 468:541–556.

76. Swartz DA, et al. (2005) The Herbig Ae star HD 163296 in X-rays. *The Astrophysical Journal* 628:811–816.

77. Günther HM, Schmitt JHHM (2009) The enigmatic X-rays from the Herbig star HD 163296: Jet, accretion, or corona?. *Astronomy and Astrophysics* 494:1041–1051.

78. Testa P, Huenemoerder DP, Schulz NS, Ishibashi K (2008) X-ray emission from young stellar objects in the ε Chamaeleontis group: the Herbig Ae star HD 104237 and associated low-mass stars. *The Astrophysical Journal* 687:579–597.